Impact of Window Temperature Variations on ITER Toroidal Interferometer and Polarimeter (TIP) Measurements

T. Akiyama[1], M.A. Van Zeeland[1], D.K. Finkenthal[2], M. LeSher[1], R. Finden[1], P. Trost[1], A. Gattuso[1], S. Miranda[2], M. Groh[1], Marc-André de Looz[3], and C. Watts[4]

[1] General Atomics, San Diego, USA
[2] Palomar Scientific Instruments, San Marcos, USA
[3] Princeton Plasma Physics Laboratory, Princeton, USA
[4] ITER Organization, Saint Paul Lez Durance, France

E-mail: akiyamat@fusion.gat.com

Received xxxxxx
Accepted for publication xxxxxx
Published xxxxxx

Abstract

The Toroidal Interferometer and Polarimeter (TIP) is one of the primary electron density diagnostics on ITER. To meet measurement requirements over several thousand seconds, environmental factors such as changes in the window temperature, air temperature, and humidity, which can cause uncompensated phase drifts, must be minimized. This paper reports measurements of the phase shift induced by ZnSe and BaF_2 windows as their temperature is varied utilizing the TIP prototype. To accomplish these measurements, test pieces of BaF_2 and ZnSe are placed in a small oven that is located in one leg of the 10.59/5.22 micron two-color interferometer TIP prototype. The oven temperature was varied from room temperature to ~90 ºC, which is slightly higher than the expected window temperatures on ITER. The vibration compensated phase shifts measured for these two materials are $d\phi_{vc}/dT/L$= 0.0121 and -0.275 deg./°C/cm for BaF_2 and ZnSe, respectively. From these measurements, it was concluded that temperature variations of the environmental/secondary confinement barrier window and primary vacuum window have to be suppressed within approximately 1°C and 2°C, respectively, in order to passively meet the electron density measurement requirements in ITER.

Keywords: Interferometer, Window material, ZnSe, BaF_2

1. Introduction

Interferometers provide electron density measurements and are indispensable diagnostics on fusion devices [1]. The measured electron density data are essential for control of fueling and machine protection as well as for plasma physics researches such as plasma instability and fluctuation studies. ITER will be equipped with two infrared CO_2 laser based interferometers, the Toroidal Interferometer and Polarimeter (TIP) [2][3] and Density Interferometer Polarimeter (DIP) [4][5].

While infrared laser interferometers typically have sufficient electron density resolution on present fusion devices, with plasma durations of a few seconds to tens of seconds [6][7][8][9], the phase measured with these systems can show long term drifts (“offset drift”). These drifts can be erroneously interpreted as electron density and ultimately set

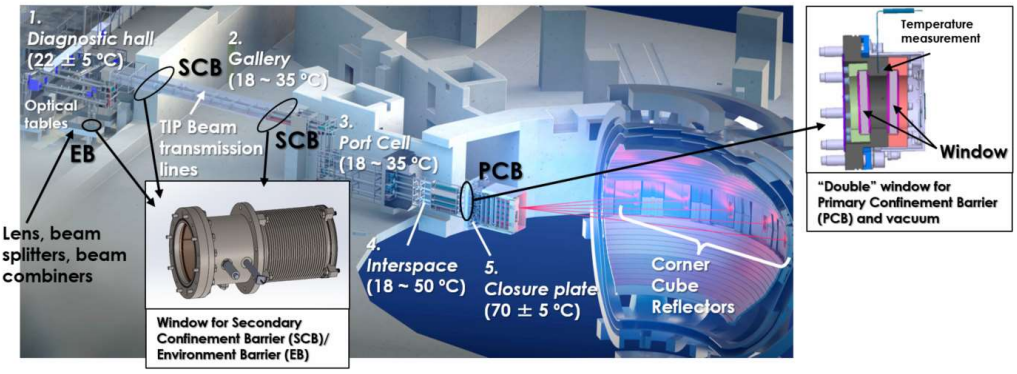

Figure 1: Transmission optics along the TIP beam relay line

the diagnostic resolution. Hence, the offset drift must be characterized and addressed for extended pulse lengths such as those expected in ITER and future steady state fusion devices.

Recent studies revealed that the offset drift is primarily caused by change of the indices of refraction of air and transmissive optics caused by environmental changes [2][10][11]. The index of refraction of air depends on humidity, temperature, and pressure whereas that of the transmissive optics depends on the temperature. Environment changes during plasma operation thus induce offset drifts, which cannot be distinguished from the plasma-induced phase. Variations of environmental factors along the beam transmission must be reduced to an acceptable level to achieve the required electron density resolution.

To specify the acceptable variation of the environmental factors for ITER TIP system, it is necessary to understand the relation between the induced phase shift and the changes in indices of refraction of air and transmission optical materials present in the system. Previous work began to quantify these effects [10][11], however, the contributions of atmospheric and transmissive components were not separated. This paper focuses on the impact of transmissive optical materials, primarily those used as windows in TIP (initially both ZnSe and BaF_2 were under consideration for primary window material with ZnSe ultimately being chosen). This provides guidelines for the mechanical and thermal designs of components related to window temperatures. The impact of air changes has been reported elsewhere, for example, in Reference [12].

Section 2 outlines two-color interferometry and the TIP optical configuration. Section 3 describes how a temperature change of transmissive material can cause uncompensated phase shifts. Based on the dependence of the index of refraction on the temperature in the presently available literature data, the phase shifts are predicted. In Section 4, the impact of window temperature changes is characterized in the TIP prototype and comparison with the predicted values is made. Additionally, these values are used to define an acceptable temperature change of the transmissive components, below which passive mitigation of phase errors is possible. Section 5 summarizes this paper.

2. Outline of TIP

2.1. Two-color interferometry

The phase shift, ϕ, measured by an interferometer traversing a plasma is caused by the plasma itself and physical path length changes from mechanical vibrations, as shown in Eq. (1) [1].

$$\phi_i = r_e \lambda_i \int_0^{l_p} n_e ds + \frac{2\pi V}{\lambda_i} \quad (1)$$

Here, the classical electron radius r_e=2.82×10^{15} m, λ is the wavelength, l_p is the path length in a plasma, n_e is the electron density, V is the path length change due to the vibration. This phase shift is provided by a phase counter. To extract the plasma-induced phase shift, two-color interferometry [1] is typically used. In TIP, a CO_2 laser and Quantum Cascade Laser (QCL) are used ($i = CO_2$ and QCL). Solving simultaneous equations for CO_2 laser and QCL, the line integrated electron density is obtained as shown in Eq. (2).

$$\int_0^{l_p} \boldsymbol{n_e dl} = \frac{\boldsymbol{\lambda_{CO2}}}{\boldsymbol{r_e}\left(\boldsymbol{\lambda_{CO_2}^2} - \boldsymbol{\lambda_{QCL}^2}\right)}\left[\boldsymbol{\phi_{CO2}} - \frac{\boldsymbol{\lambda_{QCL}}}{\boldsymbol{\lambda_{CO_2}}}\boldsymbol{\phi_{QCL}}\right] \quad (2)$$

Here, $\phi_{CO2} - \frac{\lambda_{QCL}}{\lambda_{CO2}}\phi_{QCL}$ in Eq. (2) is termed the vibration compensated phase shift.

2.2. Optical configuration of the TIP system on ITER

TIP is a 5-channel interferometer and polarimeter system [2][3]. In the present TIP prototype, the wavelengths of the CO_2 laser $\boldsymbol{\lambda_{CO_2}}$ and QCL $\boldsymbol{\lambda_{QCL}}$ are 10.59 and 5.22 μm, respectively; in the actual ITER implementation the QCL will be 4.75 μm. As shown in Figure 1, the optical tables are placed in the diagnostic hall at ITER. The probe beams are sent to the tokamak through enclosed beam relay lines. Corner

Table 1: Temperature range of each area along the TIP beam relay line. The location numbers in Figure 1 and Table 1 are common.

Location		Temperature range (ºC)
1	Diagnostic hall	22 ± 5
2	Gallery	18 ~ 35
3	Port cell	18 ~ 35
4	Interspace	18 ~ 50
5	Closure plate/vacuum window	70 ± 5

cube reflectors (CCRs) in the vacuum vessel reflect the probe beams to return the beams to the diagnostic hall. The total path length is approximately 120 m for the round trip.

There are three windows along the beam line for zoning fire and radiation control areas and two vacuum windows at the vessel. An Environment Barrier (EB) window is placed at the entrance to the beam relay line, which is above the optical table. At both sides of the gallery, there are Secondary Confinement Barrier (SCB) windows. The Primary Confinement Barrier (PCB) and vacuum window, which consists of two windows for redundancy, are located on the tokamak closure plate. The material of all windows is ZnSe. The specified temperature range in each area is shown in Table 1. The table values are primarily long-term seasonal changes and heat transfer from the tokamak, which will be operated with 70 ºC cooling water. As mentioned in Sec 3.1, the window temperature change during a plasma shot leads to the offset drift. However, the window temperature variation during a plasma shot (about 400 s for a standard inductive shot and > 1,000 s for a non-inductive shot) has not yet been fully specified at this moment. According to the progress of the temperature change of each window (for example, estimation of the temperature change of the vacuum and radiation confinement window during a plasma shot requires reliable the radiation flux and ECH stray power at the window positions, and the temperature increase of the cooling water at the window position due the heat load at upstream during a shot), the acceptable temperature change determined in this paper will be used as guidelines of the beam line design and compensation methods.

3. Impact of window temperature change on the vibration compensated phase shift

3.1. Environmental impact on the phase shift

The actual phase shift measured with the interferometer will also include phase shifts from variations of air and transmissive optics (the windows), in addition to those from plasma and vibration (See Eq. (1)).

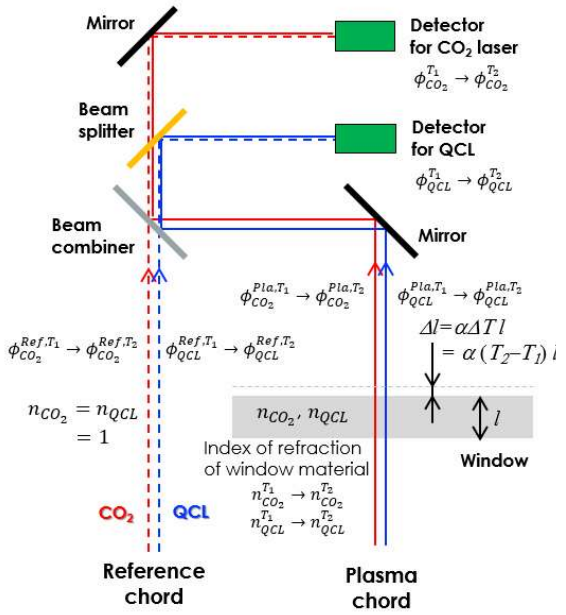

Figure 2: Conceptual beam paths of a two-color interferometer after the window.

$$\phi_i = r_e \lambda_i \int_0^{l_p} n_e ds + \frac{2\pi V}{\lambda_i} + \frac{2\pi n_{air}(\lambda_i, T, h, p)}{\lambda_i} L + \frac{2\pi n_{win}(\lambda_i, T)}{\lambda_i} l \quad (3)$$

Here, n_{air} and n_{win} are the indices of refraction for air and window material, T, h, p are the temperature, humidity, and the pressure, respectively. L is the path length in air, and l is the thickness of the window. The first and the second terms are the same as those in Eq. (1). The third and fourth terms are phase shifts in air and window, respectively, and depend on environmental factors. When the environment is static, the third and fourth terms result in a constant offset (which is subtracted off in the phase counters at t = 0). Since the line-integrated electron density is evaluated from the change in the phase after t = 0, the constant offset over the plasma shot duration does not cause any measurement error. However, when the environment changes during the plasma shot an offset drift occurs. The offset drift cannot be distinguished from the phase shift by a plasma and will lead to measurement error [2][10][11].

3.2. Phase shifts caused by thermal expansion and change of the index of refraction

Figure 2 shows the conceptual beam paths of a two-color interferometer including the window with related index of refraction and resultant phase. The phase of the measured interference signal ϕ_i is the subtraction of the phases of the

Table 2: Dependence of dn/dT on the temperature of BaF_2 and CVD ZnSe [15]

dn/dT of BaF_2 (10^{-5} /K)					
Temperature (°C)	3.39 μm	5.22 μm (interpolation)	10.6 μm	$\frac{dn_{CO_2}}{dT}-\frac{dn_{QCL}}{dT}$	Average
20	-1.59	-1.554	-1.45	0.104	0.1060
40	-1.62	-1.584	-1.48	0.104	
60	-1.66	-1.622	-1.51	0.112	
80	-1.68	-1.644	-1.54	0.104	
100	-1.71	-1.674	-1.57	0.104	
	(Standard deviation σ: 0.03)			$\sqrt{2}\sigma = 0.04$	

dn/dT of CVD ZnSe (10^{-5} /K)					
Temperature (°C)	3.39 μm	5.22 μm (interpolation)	10.6 μm	$\frac{dn_{CO_2}}{dT}-\frac{dn_{QCL}}{dT}$	Average
20	6.2	6.17	6.1	-0.075	-0.0895
40	6.2	6.17	6.1	-0.075	
60	6.3	6.25	6.1	-0.149	
80	6.3	6.27	6.2	-0.075	
100	6.3	6.27	6.2	-0.075	
	(Standard deviation σ: 0.1)			$\sqrt{2}\sigma = 0.14$	

plasma and reference chords ϕ_i^{pla} and ϕ_i^{ref}. Hence the phase of the CO_2 laser and QCL interference signal $\phi_{CO_2}^{T_1}$ and $\phi_{QCL}^{T_1}$ at initial temperature T_1 are described as

$$\phi_{CO_2}^{T_1} = \phi_{CO_2}^{Pla,T_1} - \phi_{CO_2}^{Ref,T_1} = 2\pi\frac{\left(n_{CO_2}^{T_1}-1\right)l}{\lambda_{CO_2}} \quad (4)$$

$$\phi_{QCL}^{T_1} = \phi_{QCL}^{Pla,T_1} - \phi_{QCL}^{Ref,T_1} = 2\pi\frac{\left(n_{QCL}^{T_1}-1\right)l}{\lambda_{QCL}}. \quad (5)$$

Here, $n_{CO_2}^{T_1}$ and $n_{QCL}^{T_1}$ are indices of refraction of the window material at the CO_2 laser and QCL wavelengths. Then the vibration compensated phase $\phi_{comp}^{T_1}$ at T_1 is given from Eqs. (1), (4), and (5) as below.

$$\phi_{comp}^{T_1} = \left[\phi_{co_2}^{T_1} - \frac{\lambda_{QCL}}{\lambda_{CO_2}}\phi_{QCL}^{T_1}\right] = 2\pi\frac{\left(n_{CO_2}^{T_1}-n_{QCL}^{T_1}\right)l}{\lambda_{CO_2}} \quad (6)$$

When the temperature increases by $\Delta T = T_2 - T_1$, the thickness of the window l changes to $(1+\alpha\Delta T)l$. Here, α is the thermal expansion coefficient of the window material. The index of refraction of the window material also changes according to the temperature change. The index of refraction of the window material for the CO_2 laser is given by the following Eq. (7).

$$n_{CO_2}^{T_2} = n_{CO_2}^{T_1} + \frac{dn_{CO_2}}{dT}\Delta T \quad (7)$$

At T_2, $\phi_{\mathrm{CO}_2}^{Pla,T_2}$ and $\phi_{\mathrm{CO}_2}^{Ref,T_2}$ are given as follows.

$$\phi_{CO_2}^{Pla,T_2} = 2\pi\frac{\left(n_{CO_2}^{T_1}+\frac{dn_{CO_2}}{dT}\Delta T\right)(1+\alpha\Delta T)l}{\lambda_{co_2}}$$
$$= 2\pi\frac{n_{CO_2}^{T_1}l + \frac{dn_{CO_2}}{dT}\Delta Tl + n_{CO_2}^{T_1}\alpha\Delta Tl}{\lambda_{CO_2}} + 2\pi\frac{\left(\frac{dn_{CO_2}}{dT}\Delta T\right)(\alpha\Delta Tl)}{\lambda_{CO_2}} \quad (8)$$

$$\phi_{CO_2}^{Ref,T_2} = 2\pi\frac{(1+\alpha\Delta T)l}{\lambda_{CO_2}} \quad (9)$$

For the QCL, ϕ_{QCL}^{Pla,T_2} and ϕ_{QCL}^{Ref,T_2} are obtained in the same way. When the window temperature increases to T_2, Eqs. (4) and (5) become

$$\phi_{CO_2}^{T_2} = \phi_{CO_2}^{Pla,T_2} - \phi_{CO_2}^{Ref,T_2}$$
$$= 2\pi\frac{\left(n_{CO_2}^{T_1}-1\right)l}{\lambda_{CO_2}} + 2\pi\frac{\frac{dn_{CO_2}}{dT}\Delta Tl}{\lambda_{CO_2}}$$
$$+2\pi\frac{\left(n_{CO_2}^{T_1}-1\right)\alpha\Delta Tl}{\lambda_{CO_2}} + 2\pi\frac{\left(\frac{dn_{CO_2}}{dT}\Delta T\right)(\alpha\Delta Tl)}{\lambda_{CO_2}} \quad (10)$$

$$\phi_{QCL}^{T_2} = \phi_{QCL}^{Pla,T_2} - \phi_{QCL}^{Ref,T_2}$$
$$= 2\pi\frac{\left(n_{QCL}^{T_1}-1\right)l}{\lambda_{QCL}} + 2\pi\frac{\frac{dn_{QCL}}{dT}\Delta Tl}{\lambda_{QCL}}$$
$$+2\pi\frac{\left(n_{QCL}^{T_1}-1\right)\alpha\Delta Tl}{\lambda_{QCL}} + 2\pi\frac{\left(\frac{dn_{QCL}}{dT}\Delta T\right)(\alpha\Delta Tl)}{\lambda_{QCL}} \quad (11)$$

The vibration compensated phase $\phi_{comp}^{T_2}$ at T_2 is then given by

$$\phi_{comp}^{T_2} = \left[\phi_{CO_2}^{T_2} - \frac{\lambda_{QCL}}{\lambda_{CO_2}}\phi_{QCL}^{T_2}\right] = 2\pi\frac{\left(n_{CO_2}^{T_1}-n_{QCL}^{T_1}\right)l}{\lambda_{CO_2}}$$
$$+2\pi\frac{\left(\frac{dn_{CO_2}}{dT}-\frac{dn_{QCL}}{dT}\right)\Delta Tl}{\lambda_{co_2}} + 2\pi\frac{\left(n_{CO_2}^{T_1}-n_{QCL}^{T_1}\right)\alpha\Delta Tl}{\lambda_{CO_2}}$$
$$+2\pi\frac{\left(\frac{dn_{CO_2}}{dT}-\frac{dn_{QCL}}{dT}\right)\Delta T(\alpha\Delta Tl)}{\lambda_{CO_2}}. \quad (12)$$

The change in vibration compensated phase $\phi_{comp}^{T_1\to T_2}$ caused by the temperature change from T_1 to T_2 is given by the following expression.

$$\phi_{comp}^{T_1\to T_2} = \phi_{comp}^{T_2} - \phi_{comp}^{T_1}$$
$$= 2\pi\frac{\left(\frac{dn_{CO_2}}{dT}-\frac{dn_{QCL}}{dT}\right)\Delta Tl}{\lambda_{CO_2}} + 2\pi\frac{\left(n_{CO_2}^{T_1}-n_{QCL}^{T_1}\right)\alpha\Delta Tl}{\lambda_{CO_2}}$$
$$+2\pi\frac{\left(\frac{dn_{CO_2}}{dT}-\frac{dn_{QCL}}{dT}\right)\Delta T(\alpha\Delta Tl)}{\lambda_{CO_2}} \quad (13)$$

The first, second, and third terms correspond to a phase shift caused by the difference of the dependence of the index of refraction on the temperature between two wavelengths, the thermal expansion, and coupling of these two effects.

3.3. Expected phase shifts

The published thermal expansion coefficient $\boldsymbol{\alpha}$ of BaF_2 and ZnSe are 18.1 [13] and 7.57×10^{-6} 1/°C [14], respectively. Table 2 shows the temperature derivative of the index of refraction $\frac{\boldsymbol{dn}}{\boldsymbol{dT}}$ of BaF_2 and ZnSe from Reference [15]. Since $\frac{\boldsymbol{dn}}{\boldsymbol{dT}}$

at a wavelength at 5.22 μm has not been reported in [15], it was obtained by interpolation from those at 3.39 and 10.6 μm. Since $\frac{dn_{CO_2}}{dT} - \frac{dn_{QCL}}{dT}$ depends on temperature, average values in the T = 20-100 °C range are used in the following analysis. Since each measured $\frac{dn}{dT}$ has a measurement error $\pm\sigma$ as shown in Table 2, the error in $\frac{dn_{CO_2}}{dT} - \frac{dn_{QCL}}{dT}$ is given by $\pm\sqrt{\sigma^2 + \sigma^2} = \pm\sqrt{2}\sigma$. As shown in Table 2, the signs of $\frac{dn_{CO_2}}{dT} - \frac{dn_{QCL}}{dT}$ of BaF_2 and ZnSe are opposite, which results in a large difference of the total phase shift by the temperature change between BaF_2 and ZnSe. Figure 3 shows the predicted phase shift by temperature change described by Eq. (13) using the values in Table 2. The coupling term shown in the third figure from the top (green trace) is negligible, compared to the other two terms. While phase shifts by index of refraction change and by thermal expansion largely cancel each other in BaF_2, they do not in ZnSe. Therefore, the total phase shift in ZnSe becomes larger than that of BaF_2.

4. Experimental characterization of the phase shift by window temperature change measured with TIP prototype

4.1. Experiment setup

Figure 4 shows the setup of phase shift measurement by temperature change of the window materials with the TIP prototype. As described in Sec. 2.2, this is a two-color heterodyne interferometry setup with probe beams of wavelengths of 10.59 μm and 5.22 μm. The present TIP prototype was transferred from DIII-D [3] for further bench testing. The arrangement of the lasers and optics on the optical table are basically the same as those on DIII-D [3], except no quarter-wave plate for polarimeter in these tests. A section of each window material (3 cm-thick), is put in an oven and increased the temperature up to approximately 90 °C. A thin thermocouple between the oven and the test piece measures the temperature of the window material. The oven is placed on the plasma measurement leg, and phase change by the temperature change is measured using the TIP digital phase demodulator [2][3].

4.2. Measured phase shift by temperature change of window material

Figure *5* shows the measured vibration compensated phase shifts in BaF_2 and ZnSe when the temperature is increased. While the ZnSe test piece has wedge between the laser input and output planes, the test BaF_2 piece does not. Hence intensity (not shown) and phase modulations due to the etalon effect were observed in BaF_2 as shown in Figure *5* (a-1). Since the etalon effect is caused by interference of the multi-

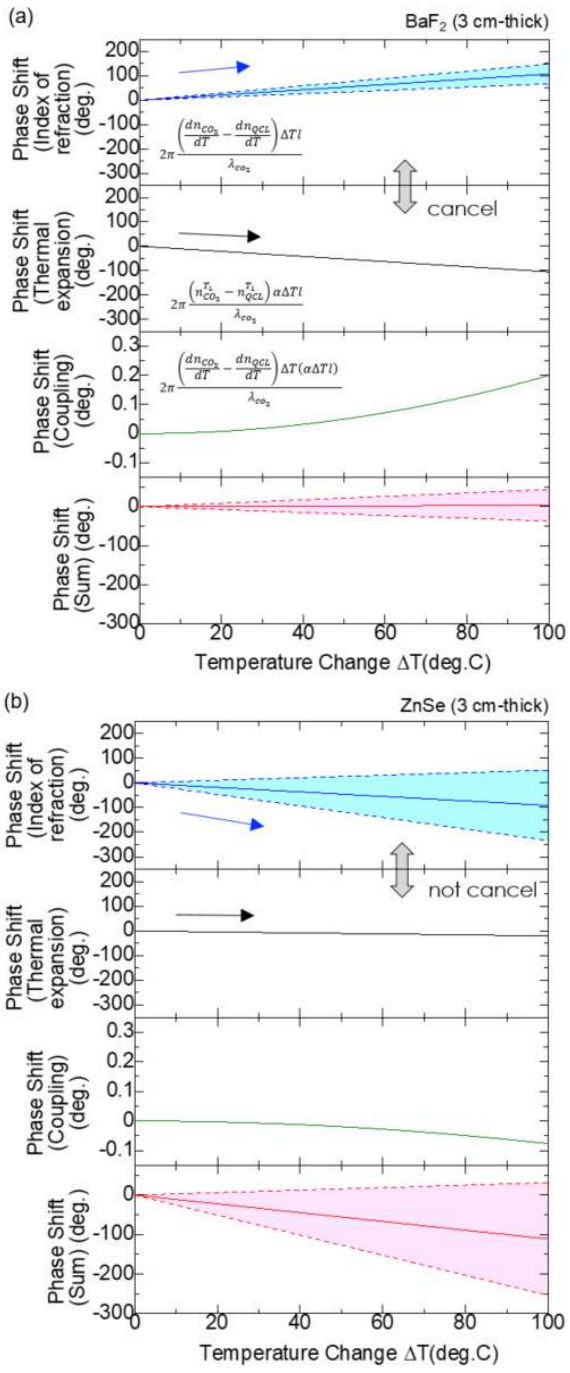

Figure 3: Predicted phase shift in 3cm-thick window materials (a) BaF_2 and (b) ZnSe caused by the temperature change ΔT. The first, second, and third figures from the top of each material are the phase shift by changes of the index of refraction, the thermal expansion, and coupling of two effects described in Eq. (13), respectively. The fourth figure is the sum of the three terms. Shaded area shows error due to the standard deviation σ of $\frac{dn}{dT}$ in Table 2.

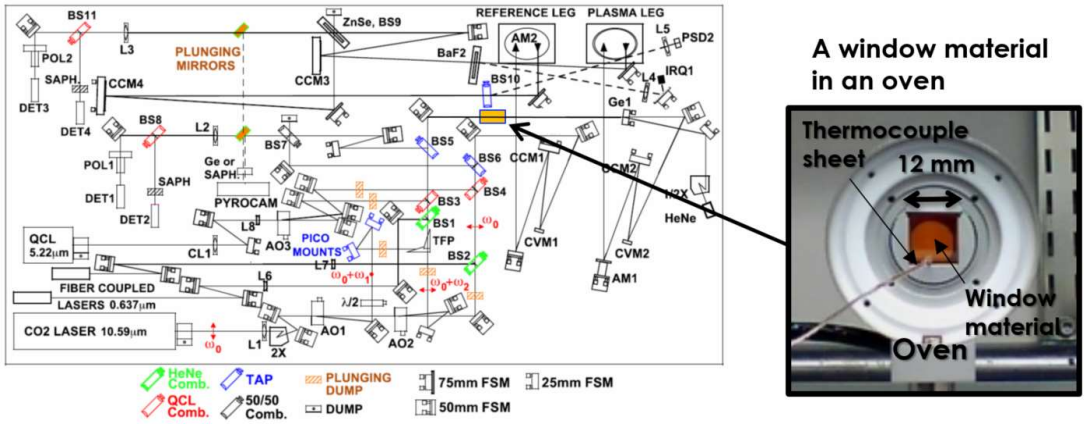

Figure 4: Position of an oven on TIP optical table and the oven with a ZnSe test piece.

reflection inside the window material, a periodic phase change as a function of the wavelength appears according to the optical path length change in the window, in addition to the linear phase change by the temperature change, which is given by Eq. (13). In order to obtain the linear relation to the temperature of BaF_2, the vibration compensated phase shift ϕ_{vc} was fitted with a function $\phi_{vc} = a\Delta T + b\sin(c\Delta T + d) + e\sin(2c\Delta T + f) + g$. Here, $b\sin(c\Delta T + d)$ and $e\sin(2c\Delta T + f)$ correspond to the etalon effects of 10.59 and 5.22 μm components, respectively. This was considered to be a best fitting, as shown in Figure *5* (a-2). Because of the wedge angle, the linear relation of ZnSe to the temperature change was easily obtained as shown in Figure *5* (b-1) and (b-2). The linear coefficients of the vibration compensated phase shift of 0.0364 and -0.824 deg./°C in 3 cm-thick BaF_2 and ZnSe test pieces are obtained, respectively, for combination of wavelengths of 10.59 and 5.22 μm (0.0121 and -0.275 deg./°C/cm for BaF_2 and ZnSe).

Figure *6* shows comparison of the predicted and measured dependence of the vibration compensated phase shift on the temperature change. The predicted values are the same as the bottom plots in Figure 3 (a) and (b). The measured phase shifts of both BaF_2 and ZnSe show good agreement with predictions calculated from published indices of refraction and their temperature dependencies to within the errors shown as shaded area.

4.3. Expected phase shift in ITER ZnSe windows by temperature change

BaF_2 is an attractive optical material because the sensitivity to the temperature change is one order of magnitude smaller than that of ZnSe as confirmed in this work. The Verdet constant, which indicates amount of Faraday rotation in a material under the magnetic field, is also smaller than ZnSe. This reduces the error of the TIP polarimeter, which measures the Faraday rotation in a plasma for an independent electron density measurement. ZnSe, however, is selected as a vacuum window material on ITER from the viewpoint of manufacturability of a vacuum sealing flange and robustness as a window material.

Supposing that the temperature changes of EB/SCB windows (Figure 1, thickness = 1 cm, double-pass) in the diagnostic area and gallery are 1 ºC and the primary vacuum window (Figure 1, thickness = 1.4 cm, double windows, and double-pass) is 2 ºC during a plasma discharge, the predicted uncompensated phase shifts in those windows will be -0.54 and -3.02 deg., respectively. Because there are one EB and two SCB windows, the total phase shift will be -4.64 deg. The conservative error budget of TIP is set at 10 deg. [12]. Since the target phase drifts caused by other effects such as humidity and temperature change along the beam transmission is approximately -4 deg. [16], the temperature changes of the EB/SCB and primary vacuum windows for passive mitigation should be suppressed to approximately 1 and 2 ºC, respectively. As described in Sec. 3.1, the phase shift caused by the temperature change before the plasma shot is subtracted and that does not affect the electron density evaluation. Therefore, the window temperature should be maintained within the above acceptable temperature changes during a plasma duration only described in Sec. 2.2. The PCB windows are cooled by cooling water at 70 ^{o}C and the SCB windows are located in the thermal insulation firebox, which prevents tritium leakage and spread of fire. The diagnostic hall, where the EB windows are located, is equipped with air conditioner. While these measures are effective in suppressing temperature changes, detailed thermal analysis is ongoing.

5. Summary

The Toroidal Interferometer and Polarimeter (TIP), which is a two-color interferometer and polarimeter, is one of the electron density diagnostics on ITER. For long pulse operation, the interferometer is challenged by change of the

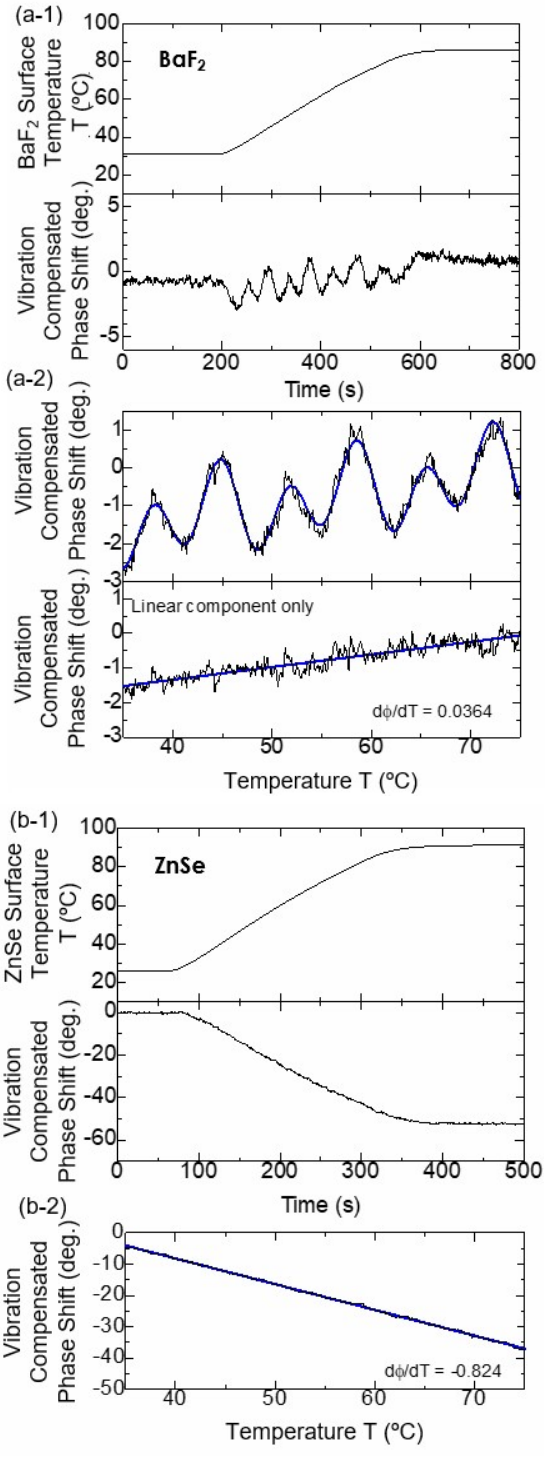

Figure 5: (a-1) The temperature and the vibration compensated phase shift of BaF_2. (a-2) The phase shift of BaF_2 as a function of the temperature and the linear component extracted by fitting. (b-1) The temperature and the vibration compensated phase shift of ZnSe. (a-2) The phase shift of ZnSe as a function of the temperature.

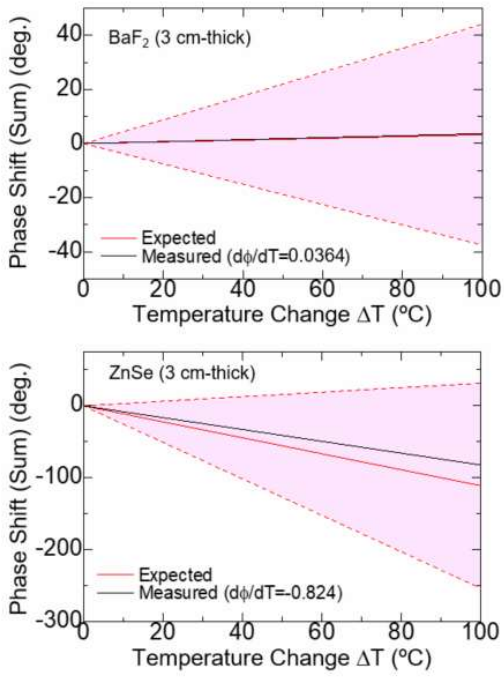

Figure 6: Comparisons between predicted and measured phase shifts by the temperature in BaF_2 and ZnSe.

phase offsets due to environmental changes such as humidity, air temperature, and temperature of transmissive optical material used for a window. The TIP prototype was utilized with an environmental control system to develop an acceptable environmental range to satisfy the required electron density resolution. The phase shift due to the temperature change of the transmission optical material is caused by the change of the index of refraction and the thermal expansion. An oven with test pieces of BaF_2 or ZnSe, typical window materials used in infrared wavelengths, was placed in the beam path of the TIP prototype; the phase shifts caused by the temperature change were then measured. The obtained dependences of the vibration compensated phase shift on the temperature for a wavelength combination of 10.59 and 5.22 μm are 0.0121 and -0.275 deg./°C/cm for BaF_2 and ZnSe, respectively. To passively satisfy electron density measurement requirements on ITER, it is necessary to suppress temperature variations within approximately 1 and 2 °C during a plasma shot by appropriate mechanical and thermal designs for the environment/secondary confinement barrier windows and primary confinement barrier and vacuum window, respectively. If temperature changes are larger than these, active phase compensation in real-time or by post process will be required. The phase offsets can be removed

through measurement of window temperature and subtraction using the values obtained here.

Acknowledgements

This work is supported by US DOE Contract No. DE-AC02-09CH11466. All US activities are managed by the US ITER Project Office, hosted by Oak Ridge National Laboratory with partner labs Princeton Plasma Physics Laboratory and Savannah River National Lab-oratory. The project is being accomplished through a collaboration of DOE Laboratories, universities and industry. The views and opinions expressed herein do not necessarily reflect those of the ITER Organization.

References

[1] D. Veron, in Infrared and Millimeter Waves ~Academic, New York, 1979, Vol. 2, pp. 67-135.
[2] M.A. Van Zeeland *et.al.*, PPCF **59**, 125005 (2017).
[3] M.A. Van Zeeland *et. al.*, Rev. Sci. Instrum. **89**, 10B102 (2018).
[4] T. Akiyama *et. al.*, Rev. Sci. Instrum. **87**, 11E133 (2016).
[5] F. Bagnato *et. al.*, JINST **20**, C03001 (2025).
[6] T.N. Carlstrom *et. al.*, Rev. Sci. Instrum. **59**, 1063 (1988).
[7] J. Irby *et. al.*, Rev. Sci. Instrum. **70**, 699 (1999).
[8] T. Kinoshita *et. al.*, Plasma Fusion Res. **17**, 1402107 (2022).
[9] Y. Ohtani *et. al.*, Rev. Sci. Instrum. **95**, 073518 (2024)
[10] K.J. Brunner *et. al.*, JINST **14**, P11016 (2019).
[11] T. Akiyama et al JINST 15 C01004 (2020).
[12] M.A. Van Zeeland *et.al.*, APS DPP Spokane, 2022
[13] https://www.crystran.co.uk/optical-materials/barium-fluoride-baf2
[14] https://ii-vi.com/product/zinc-selenide-znse/
[15] "Optical Materials Characterization Final Technical Report", NBS technical note 993, 1978
[16] TIP Preliminary Design Review, 2024